

## Natural dye extracted from *Pandanus amaryllifolius* leaves as sensitizer in fabrication of dye-sensitized solar cells

Mahmoud A. M. Al-Alwani<sup>1,4</sup>, Abu Bakar Mohamad<sup>1,3</sup>, Abd Amir H. Kadhum<sup>1</sup>, Norasikin A. Ludin<sup>2</sup>, N. E. Safie<sup>2</sup>, M. Z. Razali<sup>2</sup>, M. Ismail<sup>2</sup>, Kamaruzzaman Sopian<sup>2</sup>

<sup>1</sup> Department of Chemical and Process Engineering, Faculty of Engineering and Built Environment, Universiti Kebangsaan Malaysia, 43600 Bangi, Selangor, Malaysia

<sup>2</sup> Solar Energy Research Institute (SERI), Universiti Kebangsaan Malaysia, Bangi, 43600 Selangor, Malaysia

<sup>3</sup> Fuel Cell Institute, Universiti Kebangsaan Malaysia, Bangi, 43600 Selangor, Malaysia

<sup>4</sup> Department of Biology, College of Education for Pure Sciences/Ibn Al-Haitham, University of Baghdad, Baghdad, Iraq

\*Email address: [mamash73@yahoo.com](mailto:mamash73@yahoo.com)

Received: 25 August 2016 / Accepted: 16 November 2016 / Published: 12 December 2016

---

A dye-sensitized solar cell (DSSC) was fabricated with natural chlorophyll dye extracted from pandan (*Pandanus amaryllifolius*) leaves as natural sensitizer. Chlorophyll dye was extracted from pandan leaves using different organic solvents, namely, ethanol, acetonitrile, chloroform, ethyl ether, and methanol, to determine the effects of solvent type on the extraction. The optical and structural properties of the natural extract were also analyzed. UV-Vis spectrophotometer and Fourier transmission infrared studies (FTIR) indicated the presence of chlorophyll in pandan leaves. The absorption spectrum of the dye extract was compared with that of the dye adsorbed onto the TiO<sub>2</sub> surface. The dye structure was then confirmed through X-ray diffraction analysis (XRD). The effectiveness of electron transfer was found to be related to the interaction between the chlorophyll dye and the TiO<sub>2</sub> film surface. The morphological properties and composition of dyes were analyzed through scanning electron microscope (SEM) and EDX studies. The photovoltaic response of DSSC was investigated by recording *I*–*V* characteristics under illumination. DSSC sensitized with the pandan extract yielded the following parameters: *I*<sub>sc</sub> = 0.4 mA, *V*<sub>oc</sub> = 0.559 V, *P*<sub>max</sub> = 0.1 W, *FF* = 60.51% and *η* = 0.1%.

---

**Keywords:** DSSC, *Pandanus amaryllifolius*, chlorophyll, sensitizers, solvents

### 1. INTRODUCTION

The use of solar energy technologies has increased worldwide to provide alternative sources of energy and reduce dependence on existing energy sources [1]. Solar energy is converted into electric energy through sensitization of wide-band-gap semiconductors by using dye-sensitized solar cells

(DSSC). The production and assembly of solar cells is cost efficient and easy [2, 3]. Studies on dye sensitization focused on elucidating possible photo-sensitization reduction reactions [4]. Tsubomura used porous ZnO as the working electrode of a DSSC in 1976 and obtained a photon-electricity conversion efficiency of 2.5%; since then, DSSCs have been a subject of research on solar cells [5]. Nevertheless, the use of dye sensitization remains unsuccessful until Grätzel et al. developed a solar cell using mesoporous TiO<sub>2</sub> film in 1991 [6, 7]. DSSC has been increasingly used because it provides high energy conversion efficiency; moreover, this type of cells exhibits potential for future photovoltaic applications because of its simple fabrication process, low manufacturing cost, low environmental impact, and flexibility [8–10]. Hence, DSSC has been extensively investigated compared with conventional silicon cells [11]. Furthermore, cost optimization of solar cells has been assessed in recent decades [12]. DSSC consists of nanocrystalline porous wide band-gap semiconductor electrodes, which can absorb dyes, electrolytes (iodide and triiodide ions), and counter electrodes [13, 14].

Photo anodes are prepared through dye adsorption on the surface of the TiO<sub>2</sub> layer. The performance of DSSC is mainly determined by the type of dye used as sensitizer. The efficiency of the cell depends on the absorption spectra of the dye and its anchorage to the TiO<sub>2</sub> surface [13, 15]. Synthetic inorganic compounds (ruthenium polypyridyl complexes) are one of the most effective sensitizers because of their high conversion efficiency, excellent chemical stability, and intense charge-transfer absorption in the entire visible light spectrum [16]. However, these complexes contain metals, which are relatively expensive and hazardous to the environment [17, 18]. As such, many types of natural organic dyes extracted from leaves, fruits, and flowers of various species of plants have been actively studied and tested as low cost alternative materials to replace rare and expensive ruthenium dyes [19, 20]. Natural plant dyes can be extracted through simple procedures [6]. These dyes have been a subject of various studies because of their cost efficiency, environment friendliness, non-toxicity, availability, and full biodegradation potential [21]. Commonly studied natural dyes include chlorophyll [22, 23], anthocyanins [13, 24, 25], carotenoids [26–28], betalains [29, 30], flavonoids [31], cyanine [32], and tannins [33].

Different kinds of dyes extracted from various plant species show varied solar energy-to-electric conversion efficiencies depending on the source, chemical structure of the dyes, and degree of adsorption onto the mesoporous TiO<sub>2</sub> surface. Natural dyes as sensitizers in DSSCs perform poorly because of weak binding capabilities to the surface of the semiconductor oxide film; this phenomenon reduces excited electron transfer from the sensitizer to the conduction band of the porous film [34]. Many studies show that chlorophyll dyes are effective photosensitizer in photosynthesis and are potential environment-friendly dye sources [22]. Calogero et al. (2009) reported that the conversion efficiency of cells with chlorophyll derivatives as sensitizers is more than 2% [35], and that of cells with chlorin-e6 reaches more than 4% [36]. Chlorophyll absorbs light from red, blue, and violet wavelengths and obtains its color by reflecting green. Therefore, this pigment is a suitable photosensitizer in the visible-light region. Chlorophyll is found in the leaves of most green plants, cyanobacteria, and algae and primarily exists as chlorophyll A. Hence, from an economic point of view, chlorophyll is the optimal dye sensitizer for fabrication of DSSCs because it can be extracted through simple processes [37]. In this study, DSSCs were prepared with natural dyes extracted from

the leaves of pandan (*Pandanus amaryllifolius* L.) as photo-sensitizer. Pandan is abundant in tropical countries and has high chlorophyll content [38]. The effect of different solvents on dye extraction was investigated to determine the optimum solvent. The extracted dye was characterized using UV-Vis absorption spectrum. The performance of DSSCs containing pandan leaf extracts was also assessed.

A photosensitizer is a molecule (dye) that produces a formal change in molecule of TiO<sub>2</sub> in a photochemical process. In order to test the natural dyes as sensitizer for DSSC application, the dye sensitized solar cell was designed using *P. amaryllifolius* dye. The effective light exposure window of the DSSCs was 1cm<sup>2</sup>. The parameters of solar cell are short circuit current ( $I_{SC}$ ), open circuit voltage ( $V_{OC}$ ), fill factor ( $FF$ ), and efficiency ( $\eta$ ) and maximum power point ( $P_{max}$ ). The short circuit current and open circuit voltage are obtained from the  $I$ - $V$  curves. Also Incident Photon-to-Electron Efficiency (IPCE) was studied. The surface morphology of deposited TiO<sub>2</sub> thin film electrode was studied by scanning electron microscope. The structure of the isolated extract was studied using Fourier transmission infrared (FTIR) spectroscopy. In Addition, other confirmation that dyes supported surface of TiO<sub>2</sub>, inhibition of crystallinity of TiO<sub>2</sub> was investigated by the Energy Disperse X-ray (EDX) analysis.

## 2. MATERIALS AND EXPERIMENTS

### 2.1 Materials

The scientific classification of pandan is

Kingdom: Plantae

Order: Pandanales

Family: Pandanaceae

Genus: *Pandanus*

Species: *Amaryllifolius*

Local name: Pandan

Used part: leaves

*P. amaryllifolius* is a tropical plant widely cultivated in several countries, including Malaysia, Indonesia, Chinese, and Bangladesh; pandan leaves are widely used for cooking. This green plant has fan-shaped, blade-like leaves and very rare flowers. Studies confirmed that pandan leaves can be used as insect repellent, especially against American cockroaches (*Periplaneta americana* L.); the leaves are also used in the food industry as natural colorant [38]. Pandan contains the following aromatic compounds, namely, 2-acetyl-1-pyrroline, quercetin, tocopherols, tocotrienols, polyphenols, chlorophyll, and carotenoids [39]. Pandan is a rich source of natural green extracts [40].

### 2.2 Experimental

#### 2.2.1 Preparation of sensitizers using natural dyes

Several pieces of fresh *P. amaryllifolius* leaves were washed with distilled water and dried in an oven at 40 °C before being crushed into fine powder by using a grinder (Mulry function

disintegrator SY-04). Briefly, 25 g of the powder was immersed in 250 mL of 96% ethanol and stored for 1 week at room temperature in the dark. The extract was then filtrated using filter paper (NICE, 12.5cm, 102 Qualitative) to remove solid residues. The natural dye solution was concentrated with a rotary evaporator (Yamato RE 600) at 50 °C for 4 h. The concentrated dye extracted from pandan leaves was properly stored and protected from direct sunlight and atmospheric air. The resulting dye solution was used as sensitizer in the DSSC and then characterized.

### 2.2.2 Fabrication of dye-sensitized TiO<sub>2</sub> photo anode

TiO<sub>2</sub> porous film (photo anode) was fabricated by mixing 3.0 g of TiO<sub>2</sub> powder (anatase titanium IV oxide, ALDRICH) with 6.0 ml of 0.1 M nitric acid in a mortar and pestle. The paste was grounded completely after 30 min and added with 3.0 ml of polyethylene glycol (PEG, MW 20, 000) under continuous stirring. PEG creates a porous structure in the TiO<sub>2</sub> film, which led to high amounts of dye adsorbed on the TiO<sub>2</sub> surface. PEG also reduces crack formation, which occur during sintering at high temperatures [41]. Finally, several drops of Triton X-100 (SIGMA, for electrophoresis) were added to the mixture to facilitate the adhesion of TiO<sub>2</sub> particles to the conductive glass substrate layer [27]. Ethanol was applied on tissue to remove oil, impurities, and finger prints on the conductive glass slide. A transparent tape was used to firmly hold and prevent the sliding down of the conductive glass from the table. Furthermore, the tape controlled the thickness and the area of the TiO<sub>2</sub> film. TiO<sub>2</sub> paste was immediately spread as evenly possible onto the 1.5 cm × 1.5 cm area of the conductive glass by using a clean glass rod. After coating with TiO<sub>2</sub> for few minutes, the glass slides were sintered at 450 °C for 30 min in a furnace (LENTON THERMAL DESIGNN, England) to solidify TiO<sub>2</sub>. When cooling TiO<sub>2</sub> at about 80 °C, the film was directly immersed in the dye solution extracted from pandan leaves for 24 h at room temperature in the dark for proper adsorption of the dye on the TiO<sub>2</sub> surface. The TiO<sub>2</sub>/dye electrode was rinsed with ethanol to remove non-adsorbed dyes and excess water from porous TiO<sub>2</sub> and then dried.

### 2.2.3 Preparation of electrolyte

I<sup>-</sup>/I<sup>3-</sup> is a common electrolyte in organic solvents, such as acetonitrile, which was used in this study. Lithium ion was added to facilitate electron transport. This electrolyte is suitable for ion diffusion and infiltrates well into the TiO<sub>2</sub> film, exhibiting the highest efficiency among all DSSCs. However, the application of this electrolyte is hindered by its limited long-term stability caused by liquid volatilization. The iodide/triiodide electrolyte solution containing 0.4 M lithium iodide, 0.04 M iodine (I<sub>2</sub>), and 0.4 M tetrabutylammonium iodide was dissolved in 0.3 M N-methylbenzimidazole in a solvent mixture of 3-methoxypropionitrile and acetonitrile with a volume ratio of 1:1.

### 2.2.4 DSSC assembly

The dry TiO<sub>2</sub> porous film electrode was placed facing upward, and the conductive side of the catalyst-coated counter electrode faced the TiO<sub>2</sub> film. A DSSC was assembled by introducing liquid

electrolyte (0.5 M potassium iodide mixed with 0.05 M iodine dissolved in the solution of ethylene glycol and acetonitrile at a volume ratio 4:1) into the space between the TiO<sub>2</sub> electrode (photo anode) and the counter electrode (cathode) by capillary action. The two electrodes were clipped together using two binder clips to prevent the electrolyte from leaking.

### 2.2.5 Characterization and measurements

The absorption spectra of *P. amaryllifolius* dye solution and dye adsorbed on the TiO<sub>2</sub> surface were determined using UV-Vis spectrophotometer (Perkin Elmer, Lambda 35) in the wavelength range of 400–800 nm. The conversion efficiency of the cell was measured under irradiation (AM 1.5:100 mW/cm<sup>2</sup>). The current–voltage (*I*-*V*) curve was used to determine short-circuit current (*I*<sub>sc</sub>) and open-circuit voltage (*V*<sub>oc</sub>). The fill factor (FF) of the DSSC was calculated according to  $FF = (I_{max} \times V_{max}) / (I_{sc} \times V_{oc})$ , whereas the conversion efficiency ( $\eta$ ) of DSSC was calculated according to  $\eta = (I_{sc} \times V_{oc} \times FF) / P_{in}$ .

## 3. RESULTS AND DISCUSSION

### 3.1 Absorption wavelengths of dyes in different solvents

Fig. 1 shows the UV-Vis absorption spectra of pandan leaf extracts in ethanol, acetonitrile, chloroform, ethyl ether, and methanol. Dyes extracted from pandan leaves were soluble in ethanol as well as in the four other solvents, resulting in dark green solution. In the visible-light range, the pandan leaf extracts present a strong absorption band at about 660 nm, which is a characteristic of chlorophyll. The band for the ethanolic extract is intense and broad with a shoulder at high wavelengths.

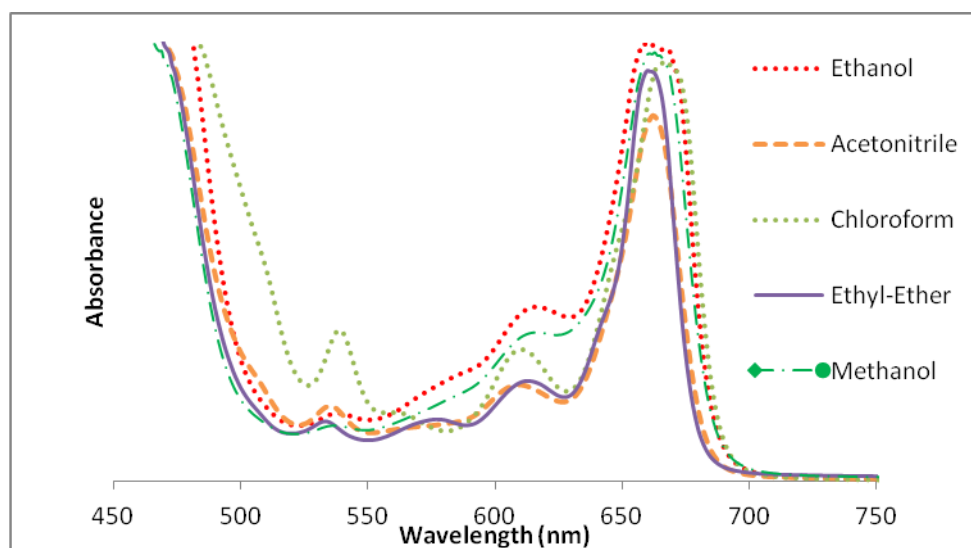


**Figure 1.** UV-Vis absorption spectra of dyes extracted from pandan leaves by using different solvents.

### 3.2 Absorption of natural dyes

Fig. 2 shows the UV-Vis absorption spectra of dyes extracted from *P. amaryllifolius*. Two main absorption peaks in the visible region were found at wavelengths of 415 and 661 nm. The broadest absorption level was detected between 400–500 nm, and the absorption range was found to be 575–700 nm. The photographic image of *P. amaryllifolius* is shown as inset in Fig. 2. The absorption spectrum for the leaf extract of *P. amaryllifolius* agrees with that of chlorophyll [6, 42]. *P. amaryllifolius* leaves contain abundant chlorophyll [8, 38]. Generally, chlorophyll exhibits an absorption band in the intense range of visible light because of charge-transfer transition from the highest occupied molecular orbital in the ground state to the lowest unoccupied molecular orbital in the excited state. Chlorophyll is a suitable material used as photosensitizer in the visible-light region [22].

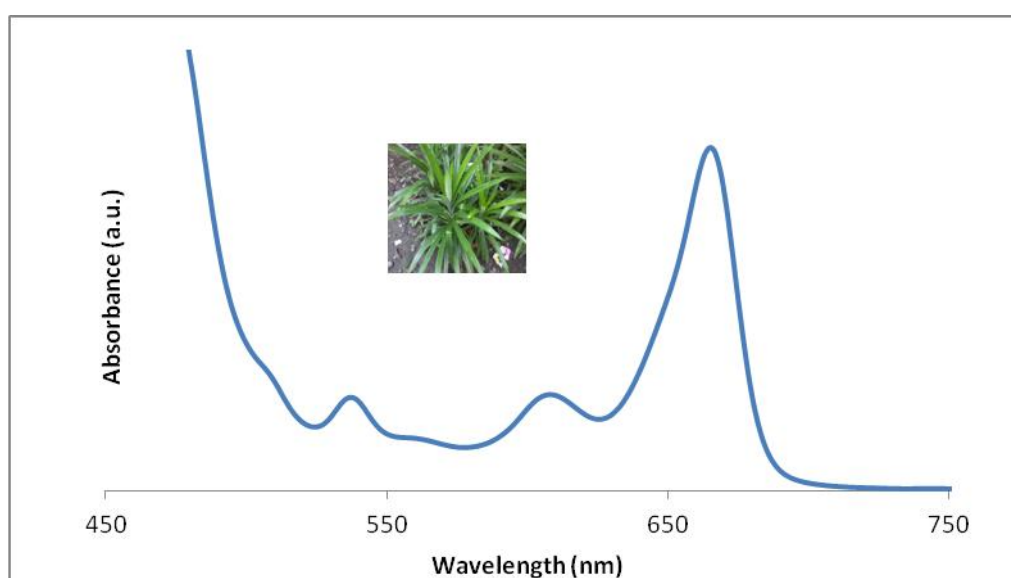


**Figure 2.** UV-Vis absorption spectrum of dye solution obtained from pandan leaves. The inset shows the photographic image of the leaves.

### 3.3 Dye structure

Fig. 3 shows that the FTIR spectrum of dye extracted from *P. amaryllifolius* leaves by using the optimal solvent (ethanol). The structure of the isolated dye was confirmed using the FTIR spectrum. The OH group appears as the broadest peak at wavelength of  $3350\text{ cm}^{-1}$ , which could be attributed to water or ethanol. The sharp peak contains three bands belonging to the C=C group, which strongly characterizes *P. amaryllifolius*. Moreover, the C=O group at  $1739\text{ cm}^{-1}$  and the CH<sub>3</sub> group at  $1456\text{ cm}^{-1}$  slightly differed in terms of transmittance intensity. The C-O group is positioned at  $1060\text{ cm}^{-1}$  as the strongest peak (sharp), indicating high amounts of dye. The aldehydes were found in wavelength between  $879\text{--}721\text{ cm}^{-1}$  emerging from the base of the organic (natural) dye.

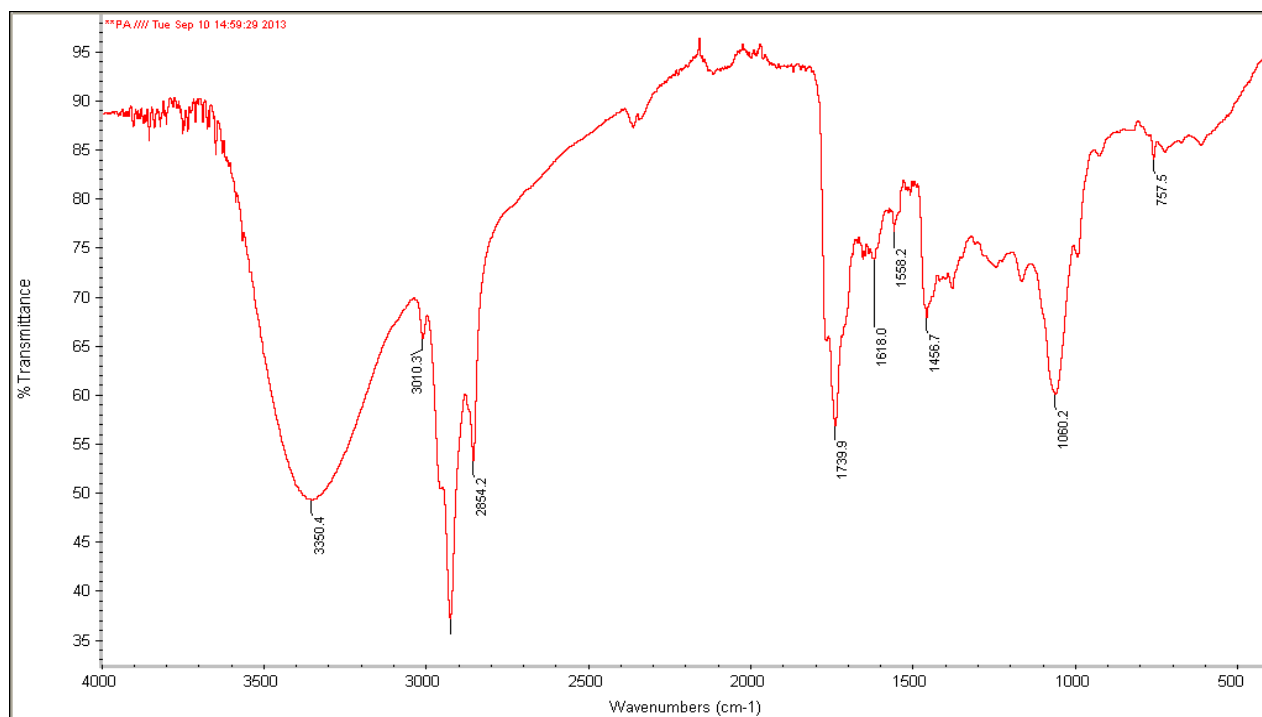


**Figure 3.** FTIR spectrum of dye obtained from *P. amaryllifolius* leaves.

### 3.4 Molecular structure of dye and dye adsorbed onto the $\text{TiO}_2$ surface

Fig. 4 presents the basic molecular structure of chlorophyll [16]. Fig. 5 compares the absorption spectrum of dye extracted from pandan leaves from that of dyes adsorbed onto the  $\text{TiO}_2$  surface. The absorption intensity of pandan leaf extracts adsorbed onto the  $\text{TiO}_2$  surface increased at wavelengths from about 400 to 700 nm; however, no significant shift was observed in the dye absorption spectrum. This finding could be due to the presence of the alkyl group rather than the hydroxyl or carboxyl group on the chlorophyll molecule, as shown in Fig 3. The presence of the alkyl group resulted in strong steric hindrance for chlorophyll to bind to  $\text{TiO}_2$  nanoparticles, thereby effectively preventing the chlorophyll molecules from arraying on the  $\text{TiO}_2$  film. This phenomenon reduced the electron transfer from the dye molecules to the conducting band of  $\text{TiO}_2$ . The experiment results are consistent with the findings reported by Hao et al. [16] and Wongcharee et al. [13].

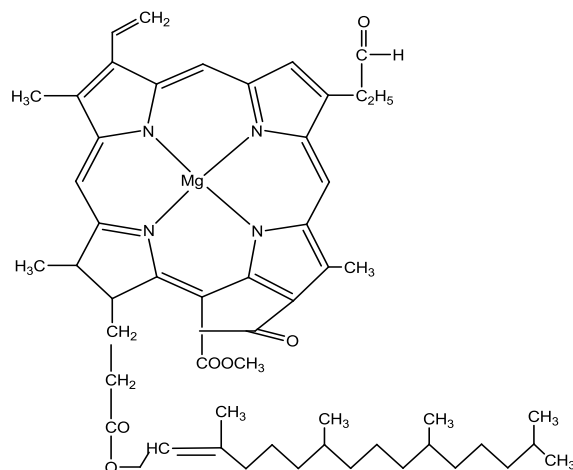


**Figure 4.** Chemical structure of chlorophyll.

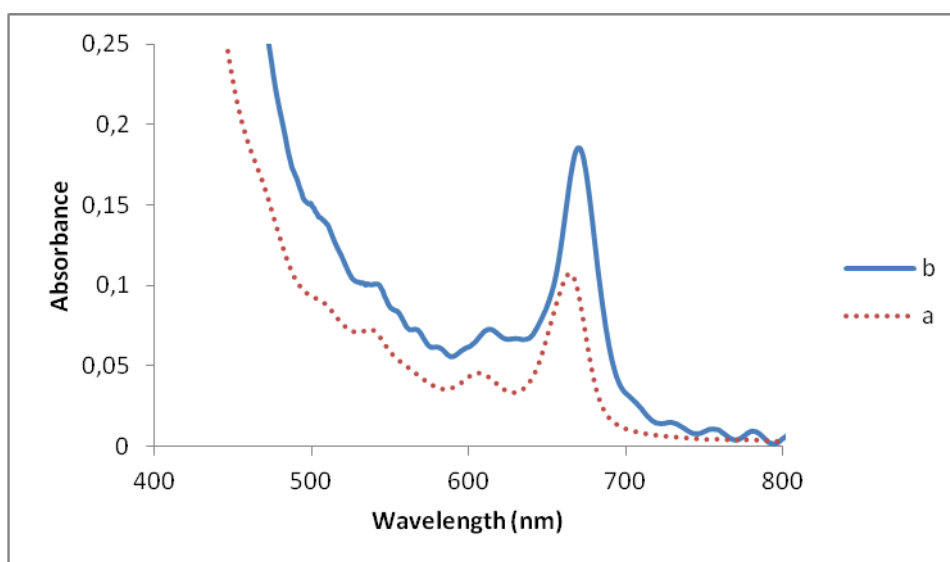


**Figure 5.** UV-Vis absorption spectrum of (a) dye solution of pandan leaves and (b) dye adsorbed on the TiO<sub>2</sub> surface.

### 3.5 Surface morphology of TiO<sub>2</sub>

The SEM image of pure TiO<sub>2</sub> shown in Fig. 6a revealed that TiO<sub>2</sub> particles aggregated to form nanoclusters; this behavior affected the photo material of DSSCs [43]. Fig. 6b shows the SEM image of natural dyes extracted from *P. amaryllifolius* after doping onto the TiO<sub>2</sub> surface. The aggregation of the TiO<sub>2</sub> particles was enhanced, and the spherical shape of the particles slightly changed because of the adsorption of chlorophyll dyes on the surface of TiO<sub>2</sub>. Aggregation of the TiO<sub>2</sub> particles could be due to uncovering of all surface particles by the dye, resulting in the attachment of the surface to the dye [44].

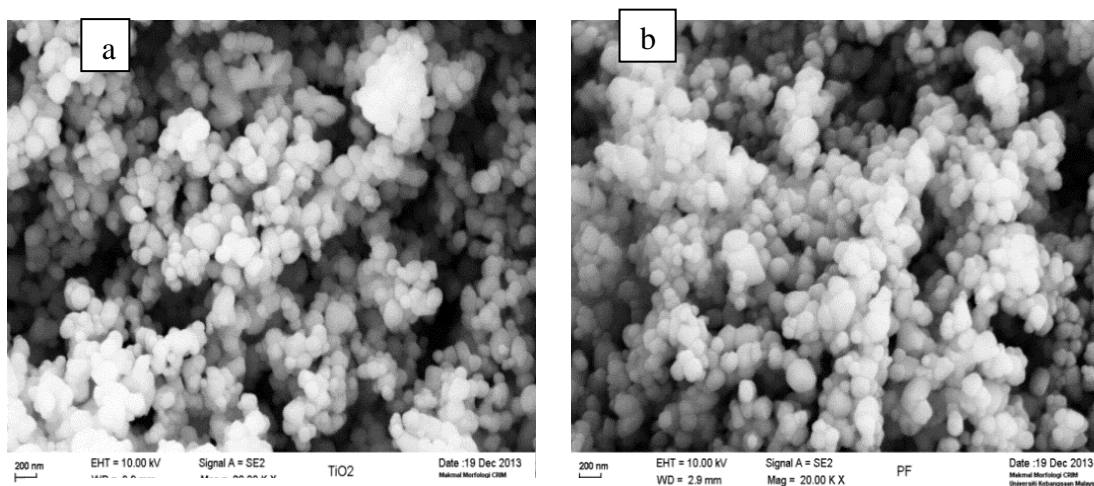


**Figure 6** SEM images of (a) pure  $\text{TiO}_2$  and (b)  $\text{TiO}_2$ -*P. amaryllifolius*.

### 3.6 EDX analysis

Fig. 7a shows the EDX spectrum of  $\text{TiO}_2$  particles. The spectra of titanium (Ti) and oxygen (O) exhibit distinguished peaks. The weight contributions of Ti and O are 52.14% and 47.85%, respectively, as presented in Table 1. This finding confirms the high purity of  $\text{TiO}_2$  particles, which will be used as photo material with natural dyes [44]. The EDX spectrum of  $\text{TiO}_2$  particles coated with *P. amaryllifolius* extract is shown in Fig. 7b. In addition to the peaks of Ti and O, the figure shows another prominent peak of the functional group in the dye. As shown in Table 1, the weight contributions of dye functional groups are 4.99%. This result indicates the presence of the functional groups of the natural dye on the  $\text{TiO}_2$  surface, which is necessary to transfer the electrons through adsorption [34].

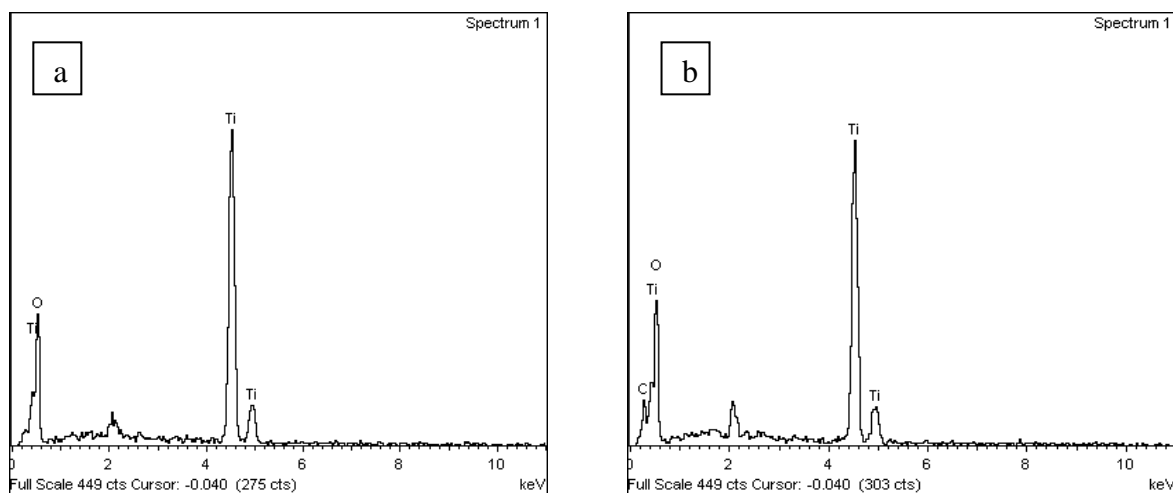


**Figure 7.** EDX spectra of (a) pure  $\text{TiO}_2$  and (b)  $\text{TiO}_2$ -*P. amaryllifolius* dye.

**Table 1.** EDX data of pure and dyed TiO<sub>2</sub>.

Pure TiO <sub>2</sub> (a)			TiO <sub>2</sub> - <i>P. amaryllifolius</i> dye (b)		
Element	Wt.%	At. %	Element	Wt.%	At. %
Ti	52.14	26.78	Ti	50	24.44
O	47.85	73.21	O	45	65.82
			C	4.99	9.73

3.7 XRD analysis

The inhibition of TiO<sub>2</sub> crystallinity was investigated through X-ray analysis, and the results are shown in Fig. 8. This finding confirms that the *P. amaryllifolius* dye was adsorbed on the surface of TiO<sub>2</sub> particles. High intensity of the main peak was observed prior to the adsorption of the chlorophyll dye on the TiO<sub>2</sub> surface (Fig. 8a). Figs 8b shows that the intensity of the main peak decreased by approximately 50% after adsorption of the *P. amaryllifolius* dye on TiO<sub>2</sub> compared with that of the peak of pure TiO<sub>2</sub> (Table 1). No peak for any dyes was observed on the XRD pattern, thereby confirming that low dye concentrations are suitable for applications because of enhanced absorption.

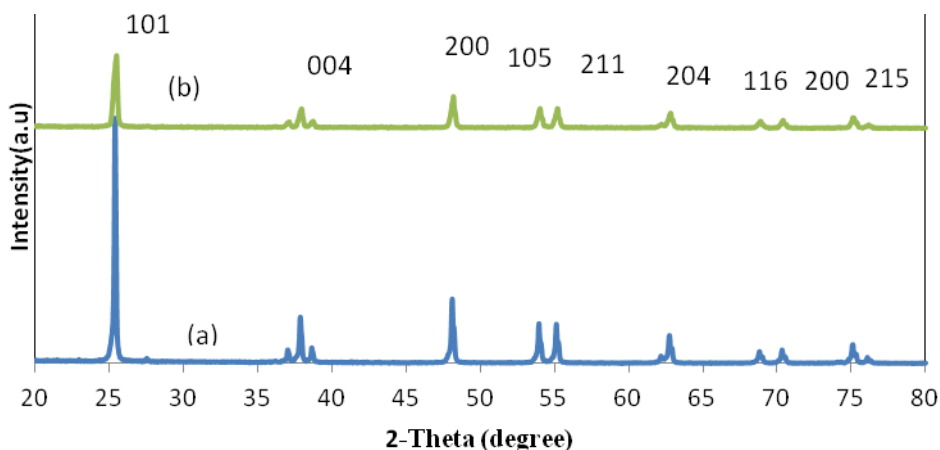


**Figure 8.** XRD of (a) pure TiO<sub>2</sub> and (b) TiO<sub>2</sub>-*P. amaryllifolius*.

**Table 2.** Intensity of all peaks of TiO<sub>2</sub> and with dyes.

Peak no. by 2θ	TiO <sub>2</sub>	TiO <sub>2</sub> + <i>P. amaryllifolius</i>
25.28	8700	3500
37.80	1700	1000
48.05	2200	1200
53.89	1400	850
55.06	1400	850
62.98	300	700
68.76	1000	300
70.31	500	400
75.03	700	500
76.02	250	250

### 3.8 Performance of DSSC sensitized with the extracted natural dye

Table 3 shows the photovoltaic test of DSSC with *P. amaryllifolius* extract as photosensitizer. The test was performed by creating the I–V curve under irradiation with white light ( $100 \text{ mW/cm}^{-2}$ ). The performance of the chlorophyll dye extracted from *P. amaryllifolius* was evaluated through analysis of open-circuit voltage ( $V_{oc}$ ), short-circuit current ( $I_{sc}$ ), fill factor ( $FF$ ), and energy conversion efficiency ( $\eta$ ). The photoelectrochemical parameters of the chlorophyll dye are summarized in Table 3, and the corresponding photocurrent–voltage curve is shown in Fig. 9. DSSC containing *P. amaryllifolius* leaf extract resulted in a fill factor of 60.51% and a maximum conversion efficiency of 0.1%.

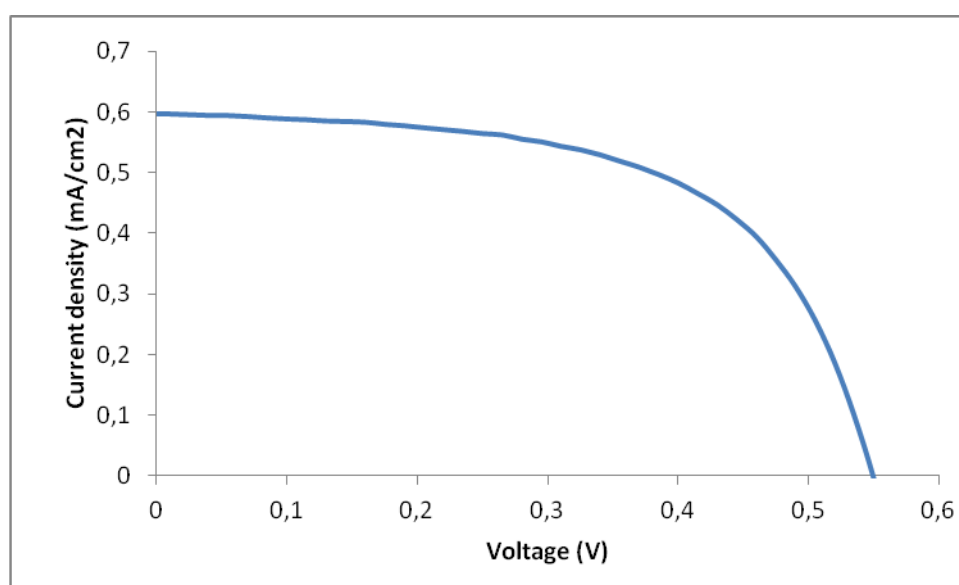


**Figure 8.** Photocurrent–voltage curve for DSSC sensitized by *P. amaryllifolius* leaf extract.

Generally, the natural dyes used as photosensitizers in DSSCs showed low conversion efficiencies compared with synthetic dyes because of the unavailability of specific functional groups [12]. Although chlorophyll plays a key role in plant photosynthesis, the process could not yield high sunlight to electricity conversion in DSSCs because of lack of available bonds between the dye molecules and the  $\text{TiO}_2$  surface for electron transportation from the excited dye to the  $\text{TiO}_2$  surface [16]. The bond and interaction between dye and  $\text{TiO}_2$  particles are important in enhancing DSSC conversion efficiency.  $V_{oc}$  (0.559 V) and  $I_{sc}$  (0.4 mA) determine the conversion efficiency of the DSSC.  $V_{oc}$  is the difference between the  $\text{TiO}_2$  Fermi level and the potential of redox electrolyte, which depends on the electron recombination rate and sensitizer adsorption mode.  $I_{sc}$  generation depends on the amount of natural dye adsorbed on the  $\text{TiO}_2$  surface; high degree of dye adsorption on the  $\text{TiO}_2$  surface generates sunlight photons that are rapidly converted into electrons, which leads to rapid injection of electrons [12, 45]. Syafinar et al. (2015) reported that the presence of Carboxyl group contained in betalains pigment extracted from *H. polyrhizus* promotes strong hydrogen bonding,

towards high characteristic [46]. Ramamoorthy et al. (2016) have used natural dyes extracted from common pear (*Opuntia dillenii*) and red tamarind (*Tamarindus indica*) to study the sensitizing efficiency in DSSCs. They found that the best conversion efficiency of 0.47 % was achieved from betalain dyes [47].

**Table 3.** Photoelectrochemical parameters of the DSSC using *P. amaryllifolius* leaf extract.

Dye	$V_{oc}$ (v)	$I_{sc}$ (mA)	$J_{sc}$ (mA/cm <sup>2</sup> )	$V_m$ (v)	$I_m$ (mA)	$P_{max}$ (W)	$\eta$ %	$FF$ %
<i>P. amaryllifolius</i>	0.55	0.4	0.4	0.428	0.3	0.1	0.1	60.51

### 3.9. Incident Photon-to-Electron Efficiency (IPCE)

In the DSSC, the large IPCE( $\lambda$ ) was related to high  $J_{sc}$  [48]. Figure 16 shows the IPCE for the DSSCs sensitized with extracts of *P. amaryllifolius*. The dye of *P. amaryllifolius* has high absorption from the incident light energy when the incident light wavelength is at the range of 300-400nm (Figure 9). The IPCE values observed at the characteristic wavelengths of the leaves dye of *C. fruticosa* was 35%. The IPCE value of dye from *P. amaryllifolius* was attributed to its broader absorption in the visible light region which is in agreement with absorption spectrum of chlorophyll dye [49]. The difference in values of IPCE of various natural dyes maybe attribute to the varied amount of dye loaded onto surface of TiO<sub>2</sub> thin film, various energy levels of excited dye molecule and the different degree of charge carrier’s recombination [50]. Calogero et al. (2012) mentioned that the nature of natural dye and dye preparation was the key factors of IPCE values [29].

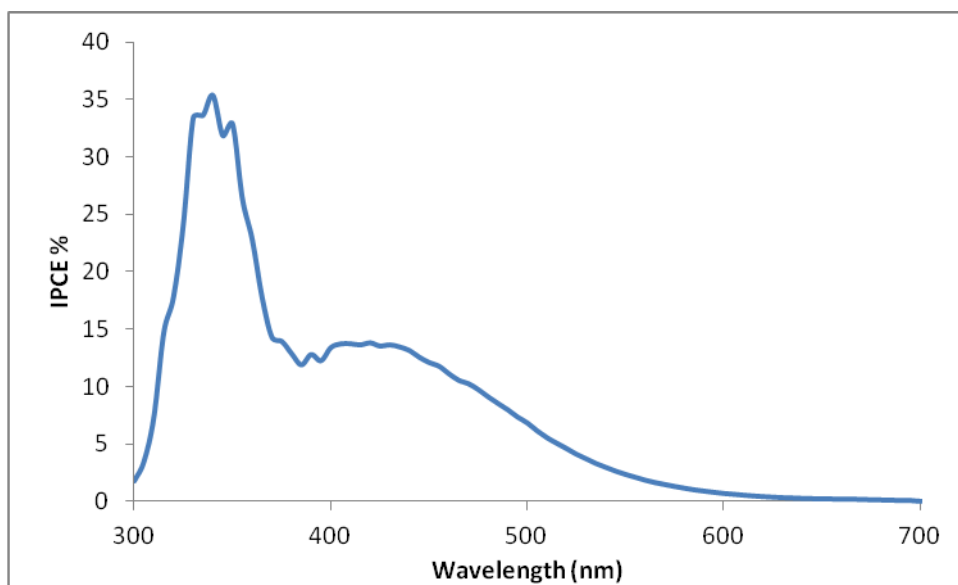


**Figure 9.** IPCE curves for the DSSCs sensitized with natural dyes from leaf of *P. amaryllifolius*

#### 4. CONCLUSION

In this paper, dyes extracted from pandan leaves (*P. amaryllifolius*) were found to be highly soluble in ethanol and soluble in acetonitrile, chloroform, ethyl ether, and methanol. The extract obtained using ethanol performed slightly better than extracts derived using the four other solvents. Chlorophyll, a natural dye obtained from pandan leaves, was used as sensitizer in DSSCs. Various photovoltaic parameters such as *I<sub>sc</sub>*, *V<sub>oc</sub>*, *P<sub>max</sub>*, *FF*, and  $\eta$  were evaluated, and the corresponding values are 0.4 mA, 0.559 V, and 0.1 W, 60.51%, and 0.1%, respectively. UV-Vis spectrophotometer and X-ray analyses were performed to confirm the adsorption of the dye on the TiO<sub>2</sub> surface. The SEM and EDX analyses were also conducted to determine the optical, structural, and morphological properties of pure TiO<sub>2</sub> and to confirm if the functional groups of the dye were attached to the TiO<sub>2</sub> surface. No significant shift was observed in the absorption spectrum after the dye was absorbed onto the surface of the TiO<sub>2</sub> film. The results obtained in dyes extracted from pandan leaves are consistent with previously reported findings.

#### ACKNOWLEDGMENTS

This study was supported by the National University of Malaysia (FRGS/1/2014/Sg06/UKM-D/P 2014) and the Solar Energy Research Institute (ICONIC-2013-006). Mahmoud A.M. Al-Alwani would like to thank the College of Education of Pure Sciences and Ibn Al-Haitham of the University of Baghdad.

#### References

1. M. Sokolsk and J. Cirák, *Materials and Processes, Acta Electrotech. Inform.*, 10 (2010) 78.
2. C.J. Barbe, F. Arendse, P. Comte, M. Jirousek, F. Lenzmanne and V. Shklover, *J. Am. Ceram. Soc.*, 80(1997)3157.
3. Y. Li, S.H. Ku, S.M. Chen, M.A. Ali and F.M.A. Alhamed, *Int. J. Electrochem. Sci.*, 8 (2013)1237.
4. C. Ruikui, Y. Xichuan, T. Haining and S. Licheng, *J Photochem. Photobiol. A Chemistry*, 189 (2007) 295.
5. H. Chang and Y. J. Lo, *Sol. Energy*, 84 (2010) 1833.
6. H. Zhou, W. Liqiong, G. Yurong and M. Tingli, *J. Photochem. Photobiol. A Chemistry*, 219 (2011) 188.
7. M. Grätzel, *J. Photochem. Photobiol. C: Photochem. Rev.*, 4 (2003) 145.
8. M.M. Noor, M.H. Buraidah, S.N.F. Yusuf, M.A. Careem, S.R. Majid and A.K. Arof, *Int. J. Photoenergy*, 2011 (2011) 5 pages.
9. D. Yu, Z. Guoliang, L. Shuang, G. Baosheng and H. Fang, *Int. J. Hydrogen Energy*, 2013 (2013) 102.
10. M.R. Narayan, *Review, Renewable Sustainable Energy Rev.* 16 (2012) 208.
11. M. Grätzel, *Nature*, 414 (2001) 338.
12. V. Shanmugan, M. Subbaiah, A. Sambandam and M. Ramaswamy, *Spectrochem. Acta, Part A*, 104 (2013) 35.
13. K. Wongcharee, V. Meeyoo and S. Chavadej, *Sol. Energy Mater. Sol. Cells*, 91 (2007) 566.
14. S. Kim, J.K. Lee, S.O. Kang, J. Ko, J.H. Yum, S. Fantacci, F.D. Angelis, D.D. Censo, M.A.K. Nazeeruddin and M. Grätzel, *J. Am. Chem. Soc.* 128 (2006) 16701.
15. M. Shahid, S. Islam and F. Mohammad, *J. Cleaner Prod.*, 53 (2013) 310.
16. S. Hao, J. Wu, Y. Huang and J. Lin, *Sol. Energy*, 80 (2006) 209.

17. H. Chang, H.M. Wu, T.L. Chen, K.D. Huang, C.S. Jwoand and Y.J. Lo, *J. Alloys Compd.*, 495 (2010) 606.
18. K.H. Park, K.T. Young, P.J. Young, J.E. Mei, Y.S. Ho, C.D. Young and L.T. Wook, *Dyes Pigm.*, 96 (2013) 595.
19. L.L. Tobin, T. O'Reilly, D. Zerulla and J.T. Sheridan, *Optik - International Journal for Light and Electron Optics*, 122 (2011) 1225.
20. M.A.M. Al-Alwani, A.B. Mohamad, A.A.H. Kadhum and N.A. Ludin, *Asian J. Chem.*, 26(2014) 6285.
21. S. Furukawa, H. Iino, T. Iwamoto, K. Kukita and S. Yamauchi, *Procedia chem.*, 518 (2009) 526.
22. C.G. Kuo, J. S. Bee and J. Chin. *Chem. Soc.*, 58 (2011) 186.
23. G. Calogero, G.D. Marco, S. Cazzanti, S. Caramori, R. Argazzi, A.D. Carlo, and C.A. Bignozzi, *Int. J. Mol. Sci.*, 11 (2010) 254.
24. P. Luo, H. Niu, G. Zheng, X. Bai, M. Zhang and W. Wang, *Spectrochim. Acta Part A*, 74 (2009) 936.
25. E.M. Abdou, H.S. Hafez, E. Bakir and M.S.A. Abdel-Mottaleb, *Spectrochim. Acta Part A*, 115 (2013) 202.
26. K.V. Hemalatha, S.N. Karthick, C.J. Raj, N.Y. Hong, S.K. Kim and H.J. Kim, *Spectrochim. Acta Part A*, 96 (2012) 305.
27. E. Yamazaki, M. Murayama, N. Nishikawa, N. Hashimoto, M. Shoyama and O. Kurita, *Sol. Energy*, 81 (2007) 512.
28. K. Yasushi, K. Yoshinori and N. Hiroyoshi, *Molecules*, 17 (2012) 2188.
29. G. Calogero, J.H. Yum, A. Sinopoli, G.D. Marco, M. Grätzel and M.K. Nazeeruddin, *Sol. Energy*, 86 (2012) 1563.
30. O.P.S. Rebecca, A. N. Boyce and S. Chandran, *Afr. J. Biotechnol.*, 9 (2010) 1450.
31. J.P.J. Marais, B. Deavours, R.A Dixon and D. Ferreira, *Springer, Columbus, Ohio, USA*, 2006, p. 1-46.
32. P.M. Sirimanne, M.K.I. Senevirathna, E.V.A. Premalal, P.K.D.D.P. Pitigala, V. Sivakumar and K. Tennakone, *J. Photochem. Photobiol. A*, 77 (2006) 324.
33. R. Espinosa, I. Zumeta, J.L. Santana, F. Martinez-Luzardo, B. Gonzalez, S. Docteur and E.Vigil, *Sol. Energ. Mat. Sol. Cells*, 85 (2005) 359.
34. N.A. Ludin, M.A.M. Al-Alwani, A.B. Mohamad, A.A.H. Kadhum, K. Sopian and N.S. Abdul-Karim, *Renewable Sustainable Energy Rev.* 31 (2014) 386.
35. G. Calogero, G.D. Marco, S. Caramori, S. Cazzanti, R. Argazzi and C.A. Bignozzi, *Energy Environ. Sci.*, 2 (2009) 1162.
36. M. Ikegami, M. Ozeki, Y. Kijitori and T. Miyasaka, *Electrochem*, 76 (2008) 140.
37. X.F. Wang, J. Xiang, P. Wang, Y. Koyama, S. Yanagida, Y. Wada, K. Kamada, S.I. Sasaki and H. Tamiaki, *Chem. Phys. Litter*, 408 (2005) 409.
38. S. Porrarud and A. Pranee, *Int. Food Research J.*, 17 (2010) 1031.
39. V. Laksanalamai and S. Ilangantileke, *Cereal Chemistry*, 70 (1993) 381.
40. U. Wissgott and K. Bortlik, *Trends Food Sci. Technol.*, 7 (1996) 289.
41. T. Pradubsang, T. Amornsakchai and U. Asawapirom, *J. Microsc. Soc. Thailand* 4 (2011) 130.
42. G.R.A. Kumara, S. Kaneko, M. Okuya, B.O. Agyeman, A. Konno and K.T. ennakone, *Sol. Energy Mater. Sol. Cells*, 90 (2006) 1220.
43. S. Ananth, T. Arumanayagam, P. Vivek and P. Murugakoothan, *Optik - International Journal for Light and Electron Optics*, 125 (2014) 495.
44. M.A.M. Al-Alwani, A.B. Mohamad, A.A.H. Kadhum and N.A. Ludin, *Spectrochim. Acta Part A*, 138 (2015) 130.
45. R. Jose, V. Thavasi and S. Ramakrishna, *Journal of the American Ceramic Society* 92 (2009) 289.
46. R. Syafinar, N. Gomesh, M. Irwanto, M. Fareq, and Y.M. Irwan, *ARPN J. Eng. Appl. Scien.*, 10(2015) 1-8.

47. R. Ramamoorthy, N. Radha, G. Maheswari, S. Anandan, S. Manoharan and R.V. Williams, *J Appl Electrochem* 46(2016) 929–941.
48. W. Maiaugree, S. Lowpa, M. Towannang, P. Rutphonsan, A. Tangtrakarn, S. Pimanpang, P. Maiaugree, N. Ratchapolthavisin, W. Sang-Aroon, W. Jarernboon and V. Amornkitbamrung, *Scientific Reports* 5(2015) 15230.
49. Z. Iqbal, W.-Q. Wu, D.-B. Kuang, L. Wang, H. Meier, and D. Cao, *Dyes Pigments* 96(2013) 722.
50. R. Kushwaha, P. Srivastava and L. Bahadur, *J. Energy* (2013) 1-8.

© 2017 The Authors. Published by ESG ([www.electrochemsci.org](http://www.electrochemsci.org)). This article is an open access article distributed under the terms and conditions of the Creative Commons Attribution license (<http://creativecommons.org/licenses/by/4.0/>).